Impacts of the nuclear symmetry energy on neutron star crusts

Bao Shishao

Nankai University

20-22 Oct. 2014

QCS, KIAA, PKU, Beijing

Possible structure of a neutron star

J. M. Lattimer and M. Prakash, Science, 304, 536 (2004)

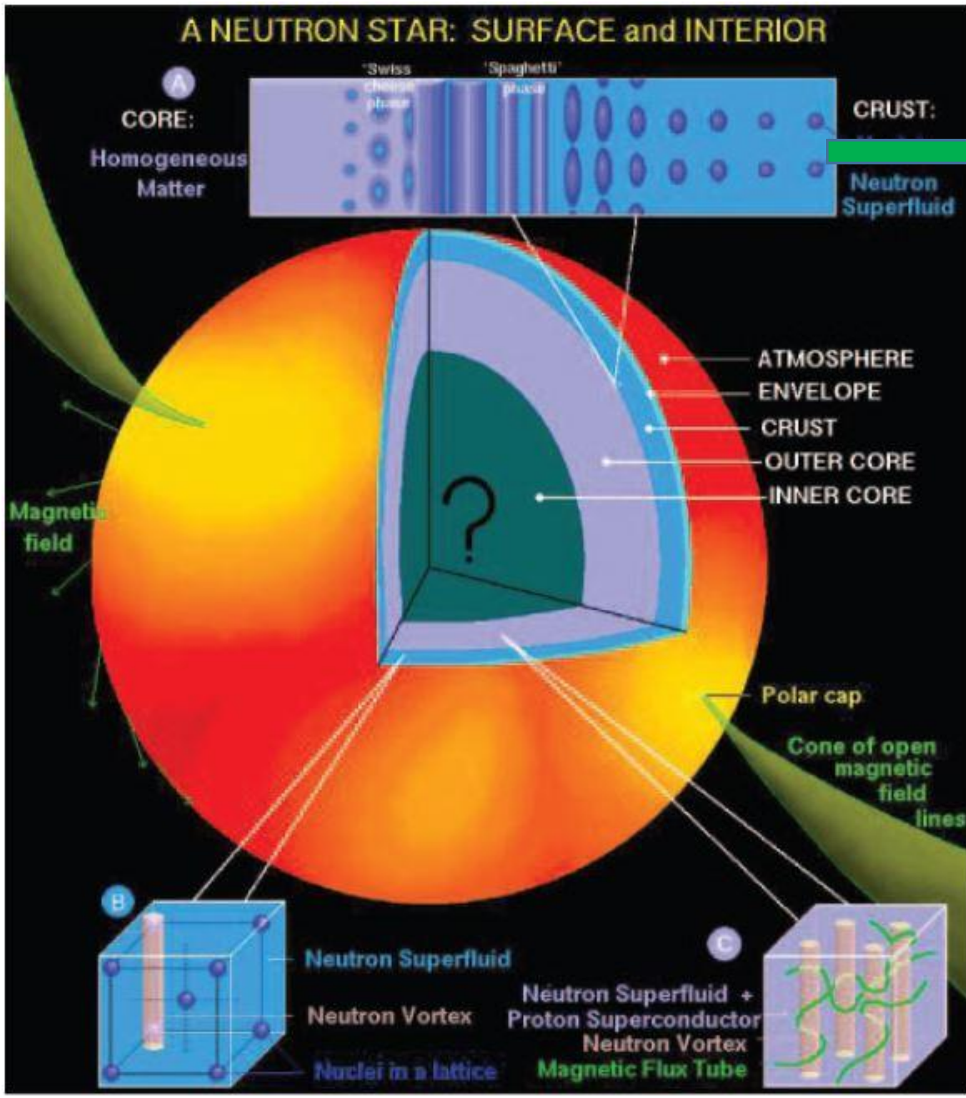

pasta

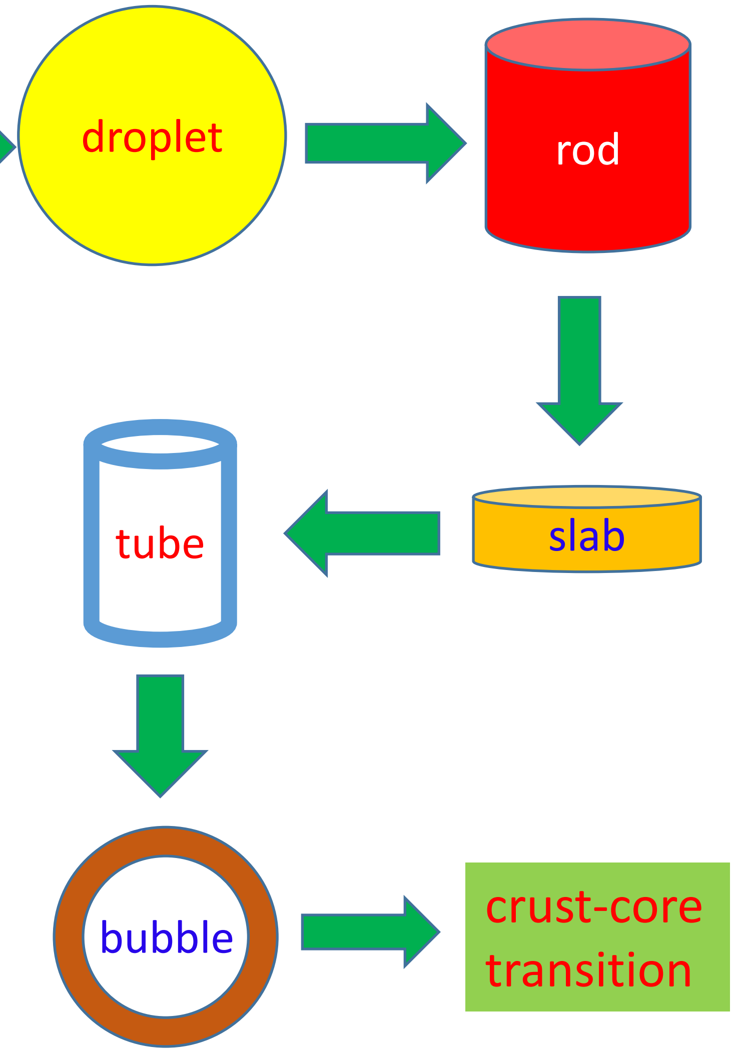

Symmetry energy

symmetry energy E_{sym} → pasta phase, crust-core transition →
- moment of inertia
- cooling
- evolution

At nuclear saturation density ($n_0 \approx 0.15\ fm^{-3}$) :

$E_{sym} = 30 \pm 4$ MeV ⟸ experiments ⟹ L=? 20 ⟺ 115 MeV

$$L = 3n_0 \left[\frac{\partial E_{sym}(n_b)}{\partial n_b}\right]_{n_b=n_0}$$

A. W. Steiner, Phys. Rev. C77, 035805 (2008).

D. G. Ravenhall, C. J. Pethick, and J. R. Wilson, Phys. Rev. Lett. 50, 2066 (1983).

Z. Zhang and L. W. Chen, Phys. Lett. B 726, 234 (2013).

Liquid drop model:

G. Watanabe, K. Iida, and K. Sato, Nucl. Phys. A 676, 455 (2000).

C. Ducoin, J. Margueron, and C. Providência, Europhys. Lett. 91, 32001 (2010).

Macroscopic model:

K. Oyamatsu and K. Iida, Phys. Rev. C 75, 015801 (2007).

Electron screening effect in pasta phase:

T. Maruyama, T. Tatsumi, D. N. Voskresensky, T. Tanigawa, and S. Chiba, Phys. Rev. C 72, 015802 (2005).

G. Watanabe and K. Iida, Phys. Rev. C 68, 045801 (2003).

Relativistic mean-field theory:

S. S. Avancini, D. P. Menezes, M. D. Alloy, J. R. Marinelli, M. M. W. Moraes, and C. Providência, Phys. Rev. C78, 015802 (2008).

S. S. Avancini, S. Chiacchiera, D. P. Menezes, and C. Providência, Phys. Rev. C 82, 055807 (2010).

F. Grill and C. Providência, Phys. Rev. C 85, 055808 (2010).

M. Okamoto, T. Maruyama, K. Yabana, and T. Tatsumi, Phys. Rev. C 88, 025801 (2013).

L ⟷ clear relation ? ⟷

pasta phases
crust-core transition

nucleon interaction:

Relativistic mean-field (RMF) theory + TM1 / IUFSU model

$$
\begin{aligned}
\mathcal{L}_{\rm RMF} \;=\; & \bar{\psi}\left[i\gamma_\mu\partial^\mu - (M+g_\sigma\sigma) - \left(g_\omega\omega^\mu + \frac{g_\rho}{2}\tau_a\rho^{a\mu}\right)\gamma_\mu\right]\psi \\
& +\frac{1}{2}\partial_\mu\sigma\partial^\mu\sigma - \frac{1}{2}m_\sigma^2\sigma^2 - \frac{1}{3}g_2\sigma^3 - \frac{1}{4}g_3\sigma^4 \\
& -\frac{1}{4}W_{\mu\nu}W^{\mu\nu} + \frac{1}{2}m_\omega^2\omega_\mu\omega^\mu + \frac{1}{4}c_3\left(\omega_\mu\omega^\mu\right)^2 \\
& -\frac{1}{4}R^a_{\mu\nu}R^{a\mu\nu} + \frac{1}{2}m_\rho^2\rho^a_\mu\rho^{a\mu} + \Lambda_{\rm v}\left(g_\omega^2\omega_\mu\omega^\mu\right)\left(g_\rho^2\rho^a_\mu\rho^{a\mu}\right)
\end{aligned}
$$

→

- Equation of motion
- Energy density
- Pressure

Adjust Λ_v, g_ρ → Fix symmetry energy at density n_{fix} → New slope of E_{sym}, L

$n_{fix}=n_0$ OK $n_{fix}=0.11\ fm^{-3}$

↓

Saturation property | Mass of PSR J1614-2230 and PSR J3048+0432 | Finite nuclei

S. S. Bao and H. Shen, Phys. Rev. C 89, 045807 (2014).

S. S. Bao, J. N. Hu, Z. W. Zhang, and H. Shen, Phys. Rev. C 90, 045802 (2014).

Parameters

$n_{fix}=n_0$

TM1

L (MeV)	50.0	60.0	70.0	80.0	90.0	100.0	110.8
g_ρ	13.8757	12.6431	11.6896	10.9237	10.2910	9.7569	9.2644
Λ_v	0.0254	0.0212	0.0171	0.0129	0.0087	0.0045	0.0000

IUFSU

L (MeV)	47.2	50.0	60.0	70.0	80.0
g_ρ	13.5899	12.6766	10.4742	9.1260	8.1926
Λ_v	0.0460	0.0433	0.0336	0.0238	0.0141

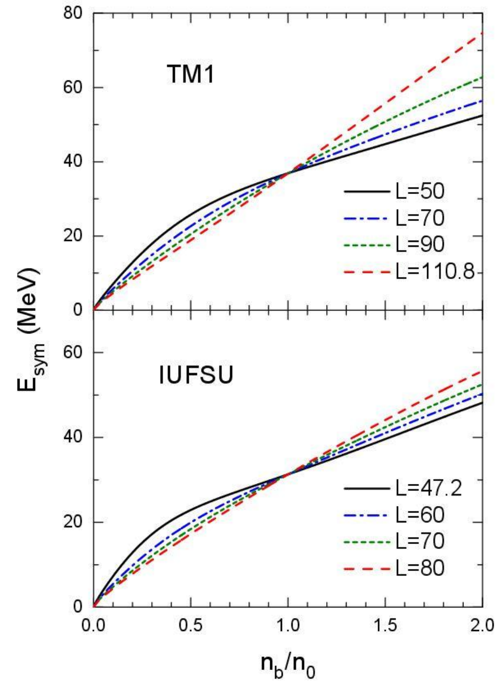

$n_{fix}=0.11$ fm^{-3}

TM1

L (MeV)	40.0	50.0	60.0	70.0	80.0	90.0	100.0	110.8
g_ρ	13.9714	12.2413	11.2610	10.6142	10.1484	9.7933	9.5114	9.2644
Λ_v	0.0429	0.0327	0.0248	0.0182	0.0128	0.0080	0.0039	0.0000

IUFSU

L (MeV)	47.2	50.0	60.0	70.0	80.0	90.0	100.0	110.0
g_ρ	13.5900	12.8202	11.1893	10.3150	9.7537	9.3559	9.0558	8.8192
Λ_v	0.0460	0.0420	0.0305	0.0220	0.0153	0.0098	0.0051	0.0011

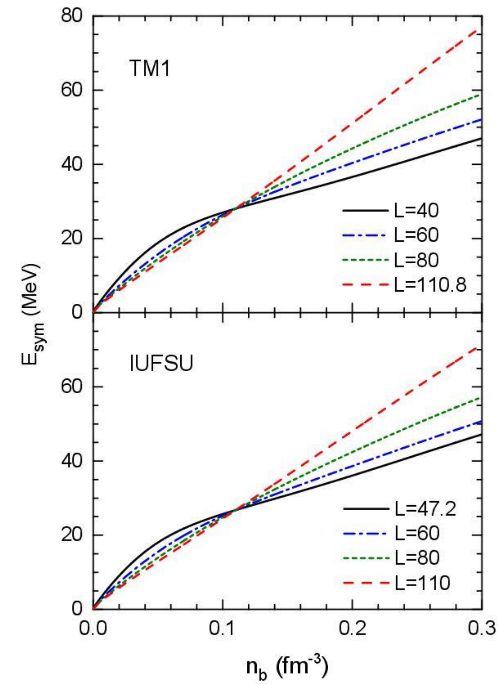

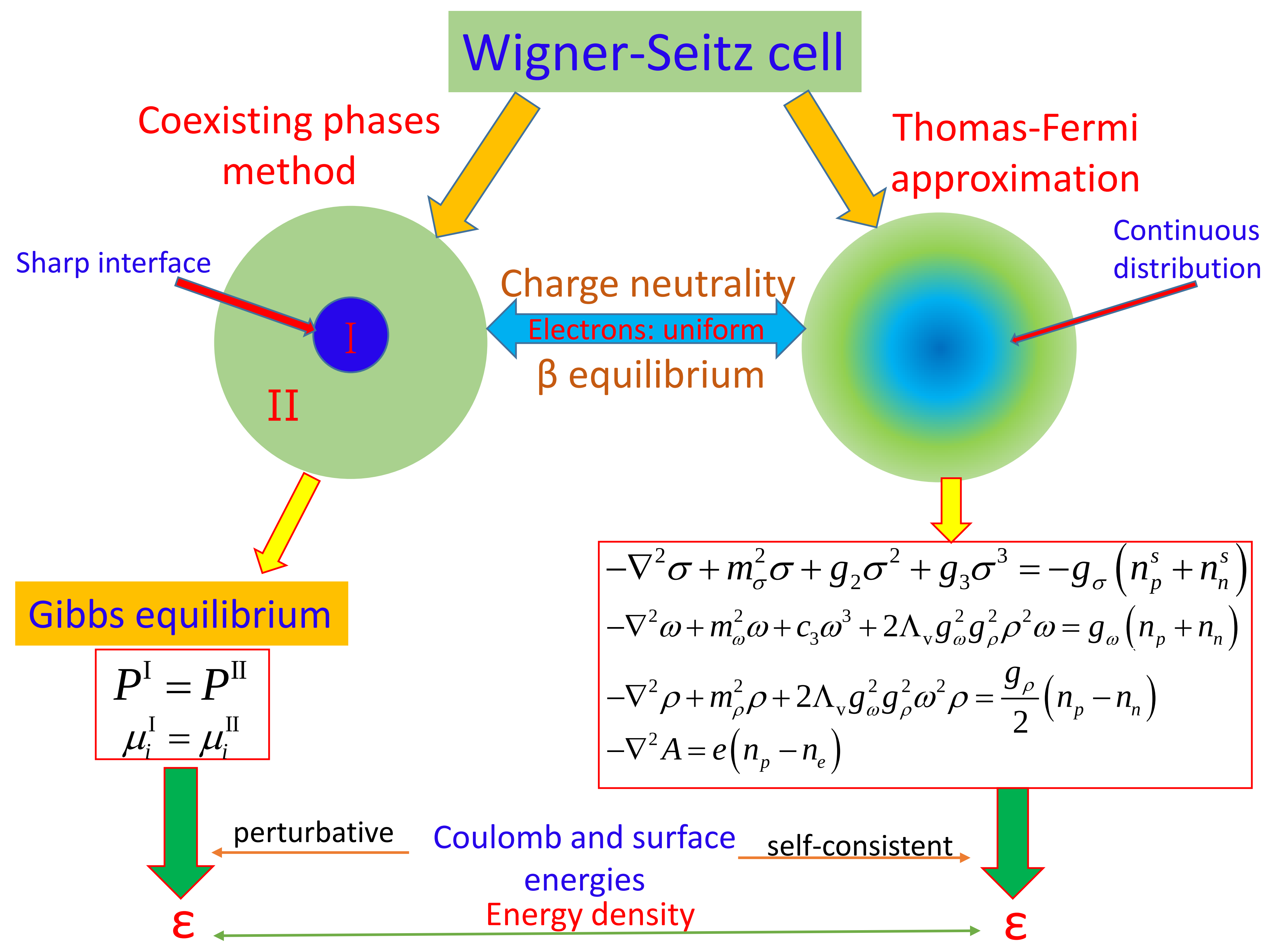

Wigner-Seitz cell
Coexisting phases method
Thomas-Fermi approximation
Sharp interface
I
II
Charge neutrality
Electrons: uniform
β equilibrium
Continuous distribution
Gibbs equilibrium
$P^{\mathrm{I}} = P^{\mathrm{II}}$
$\mu_i^{\mathrm{I}} = \mu_i^{\mathrm{II}}$
$-\nabla^2\sigma + m_\sigma^2\sigma + g_2\sigma^2 + g_3\sigma^3 = -g_\sigma\left(n_p^s + n_n^s\right)$
$-\nabla^2\omega + m_\omega^2\omega + c_3\omega^3 + 2\Lambda_v g_\omega^2 g_\rho^2\rho^2\omega = g_\omega\left(n_p + n_n\right)$
$-\nabla^2\rho + m_\rho^2\rho + 2\Lambda_v g_\omega^2 g_\rho^2\omega^2\rho = \frac{g_\rho}{2}\left(n_p - n_n\right)$
$-\nabla^2 A = e\left(n_p - n_e\right)$
perturbative
Coulomb and surface energies
self-consistent
ε
Energy density
ε

Pasta phases

Coexisting phase method

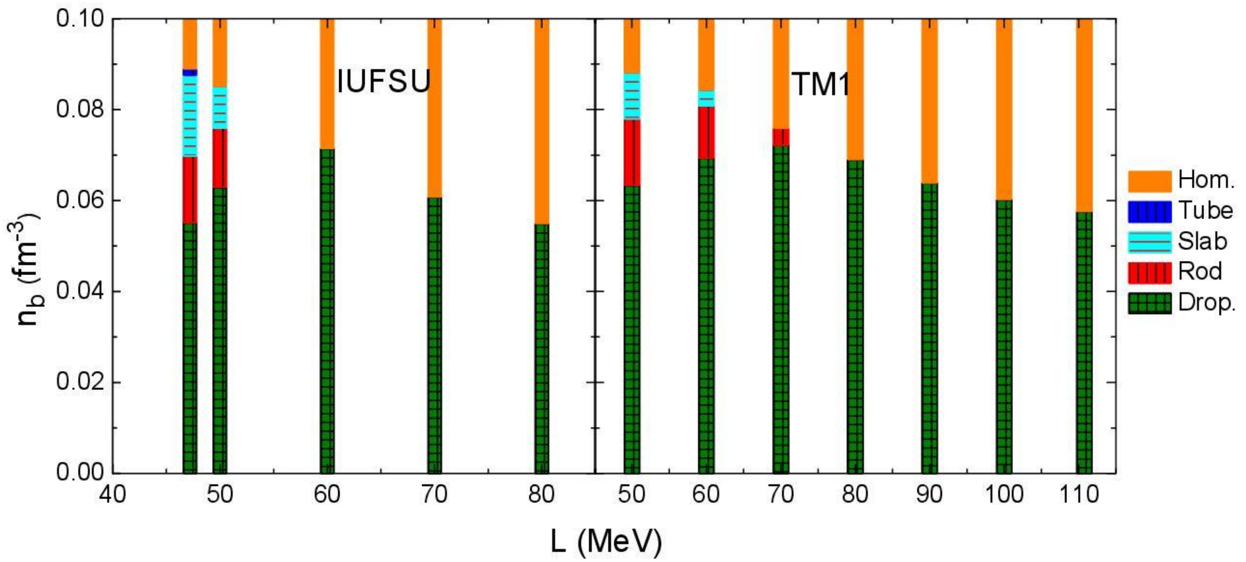

Thomas-Fermi approximation

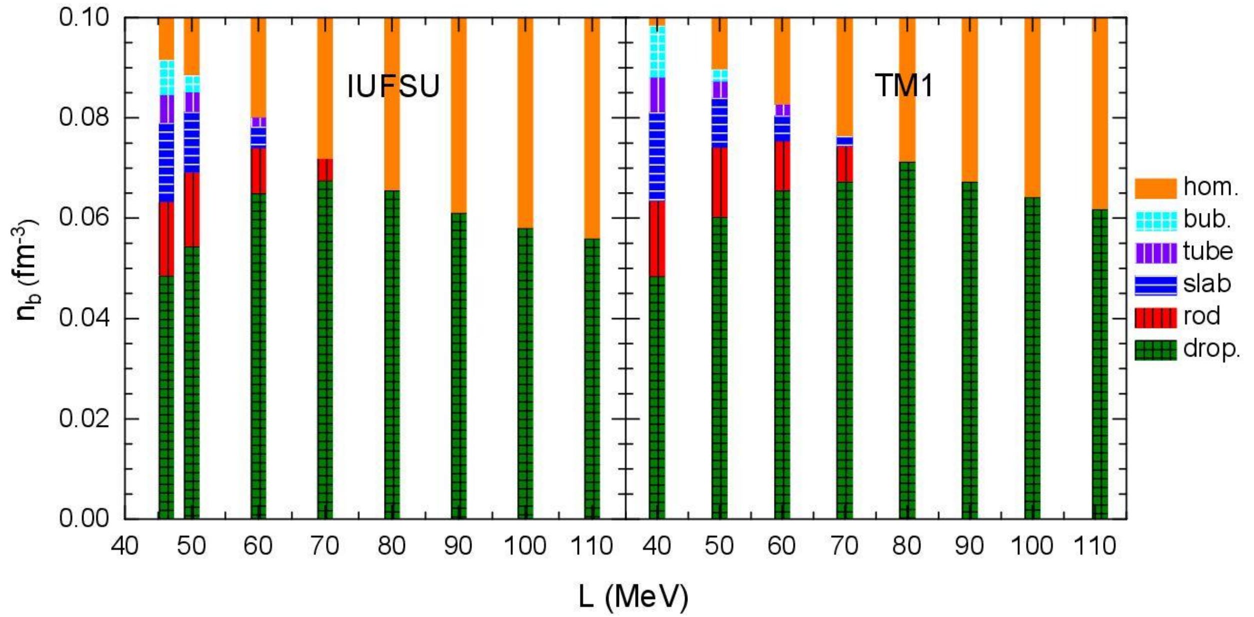

Sizes of the Wigner-Seitz cell and its dense part in Thomas-Fermi approximation

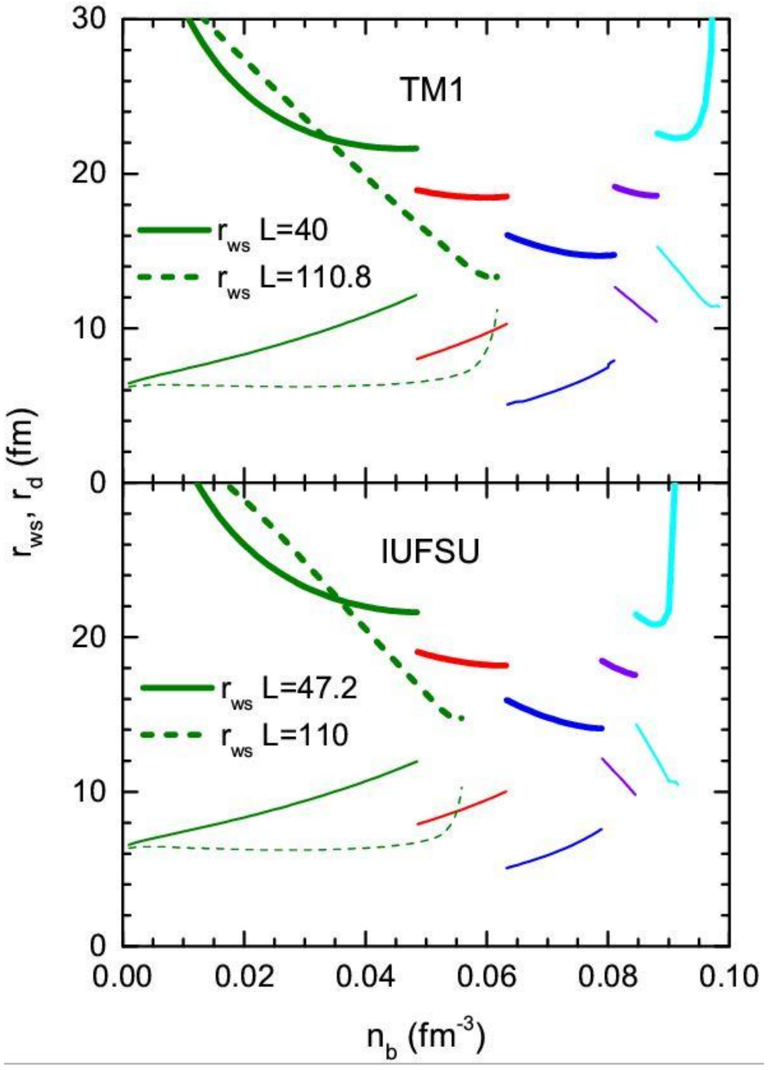

$$r_d = \begin{cases} r_{\rm ws} \left(\frac{\langle n_p \rangle^2}{\langle n_p^2 \rangle} \right)^{1/D} & \text{(droplet, rod, and slab),} \\ r_{\rm ws} \left(1 - \frac{\langle n_p \rangle^2}{\langle n_p^2 \rangle} \right)^{1/D} & \text{(tube and bubble).} \end{cases}$$

D =3, 2, 1

Proton number Z_d and nucleon number A_d of the droplet in Thomas-Fermi approximation

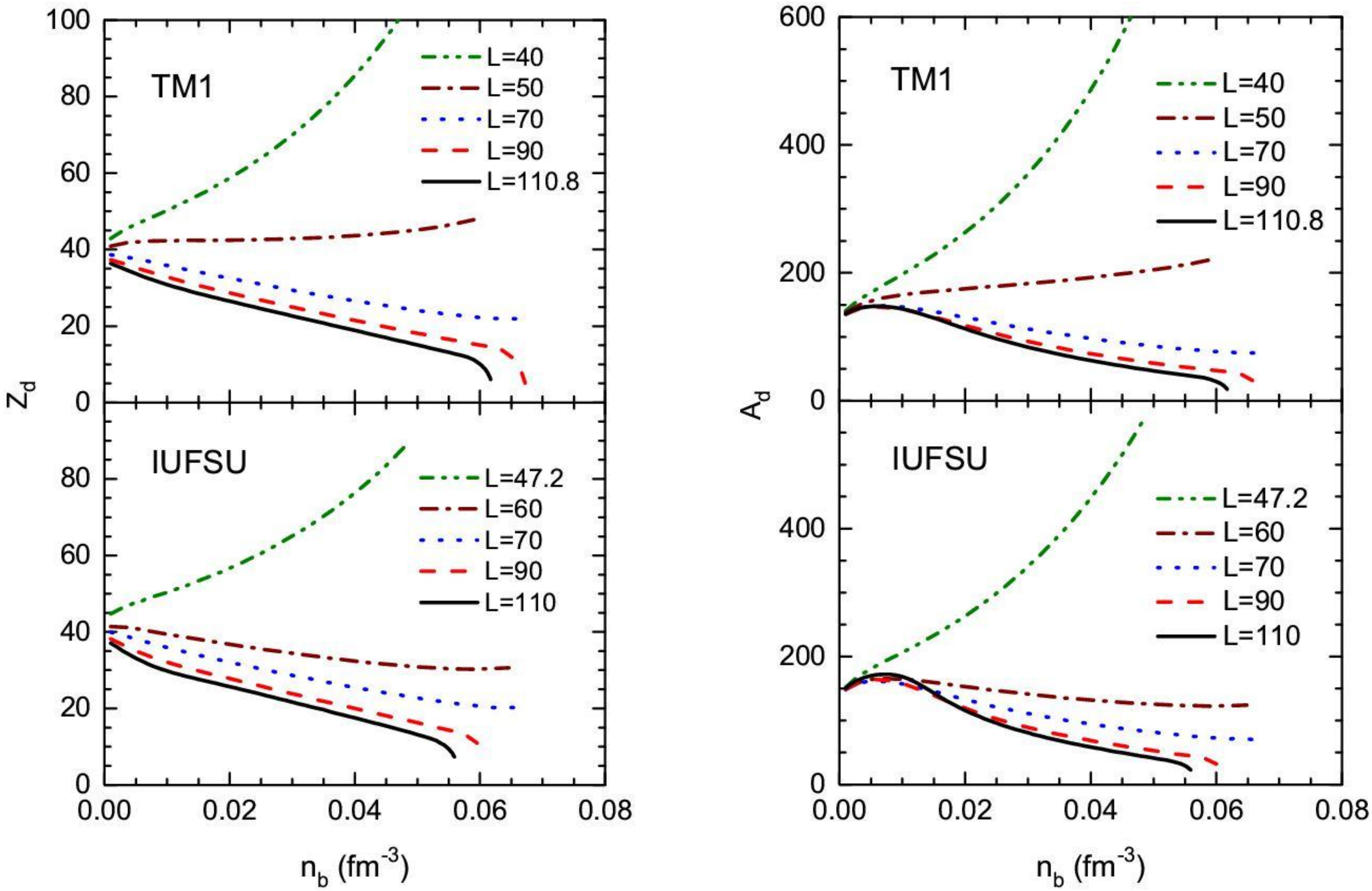

Crust-core transition properties obtained in Thomas-Fermi approximation

Baryon density

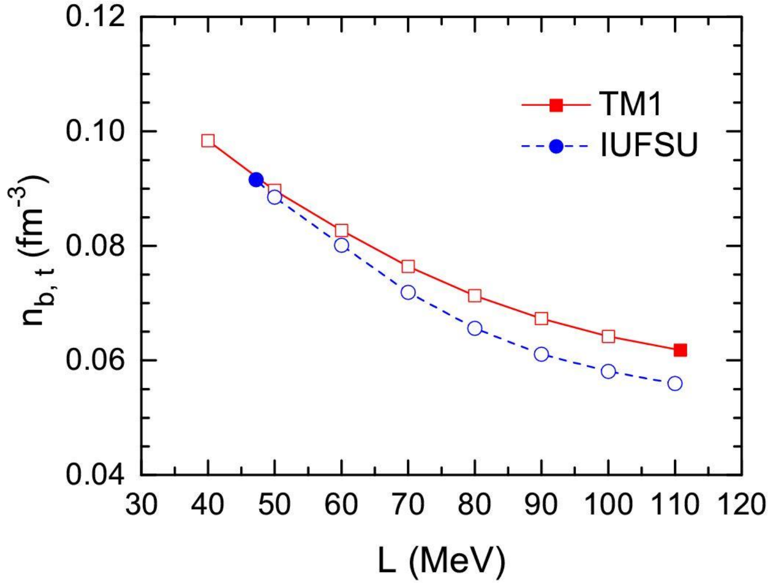

Proton fraction

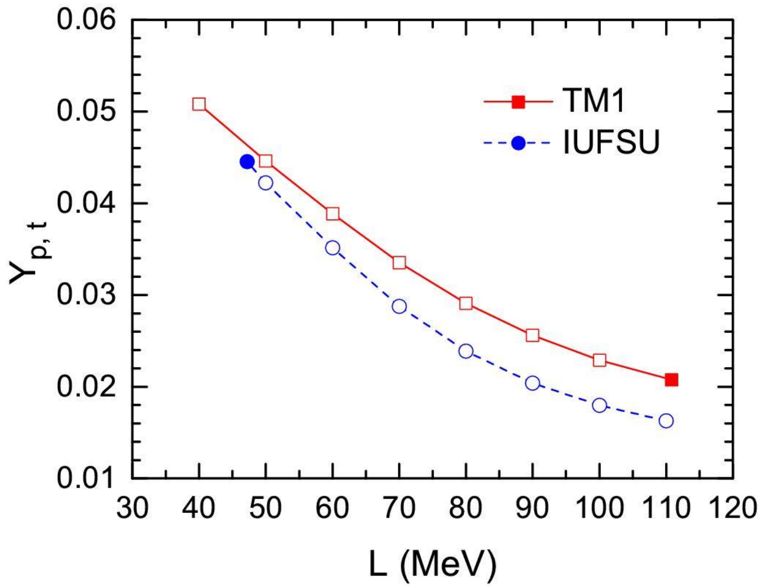

Pressure

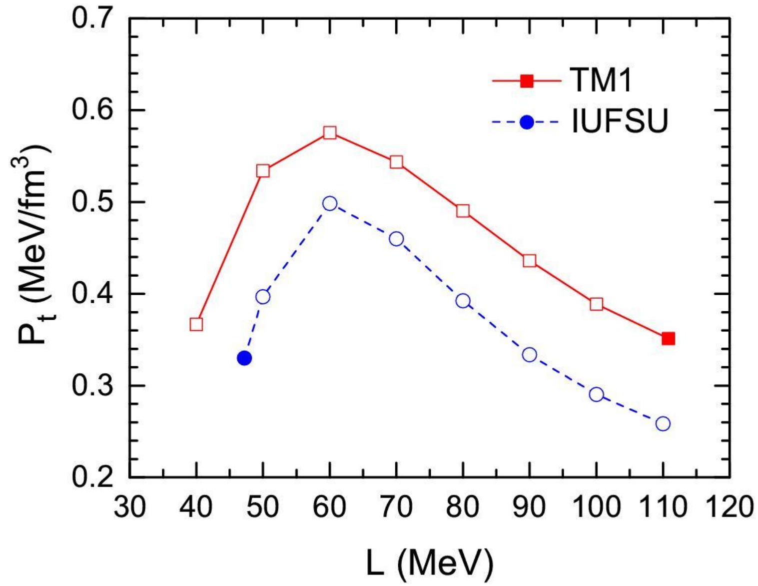

Summary

1. Within the relativistic mean-field (RMF) theory, two different methods, coexisting phase method and Thomas-Fermi approximation, are adopted to study the properties of pasta phases and crust-core transition.

2. The symmetry energy slope L plays an important role in the pasta phases and crust-core transition.

3. The main results obtained here are consistent with the ones in other methods.

4. A smaller slope L predicts more complex pasta phases and more nucleon and proton numbers in the droplet.

5. Crust-core transition density and the proton fraction at this point decrease with symmetry slope L.

6. There is no monotonic relation between symmetry slope L and the pressure at crust-core density.

? Finite temperature

Thank you!